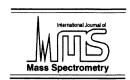


International Journal of Mass Spectrometry 177 (1998) 227-230



Subject Index

Absorption potential

Ionizing collisions of electrons with H_2O molecules in ice and in water, 137

Atomic weight

Absolute isotopic composition and atomic weight of erbium, 131

Binding energies

New evidence in favor of a high (10 eV) C_2 binding energy in C_{60} , L9

Carbon

Density functional study of mixed silicon carbide cluster cations $C_n \operatorname{Si}_p^+$ (n + p = 5,6), 31

Carbon clusters

Density functional study of mixed silicon carbide cluster cations $C_n \operatorname{Si}_p^+$ (n + p = 5,6), 31

Cations

Density functional study of mixed silicon carbide cluster cations $C_nSi_p^+$ (n + p = 5.6), 31

CCl₄

Formation mechanism of CCl₄ anion in condensed phase: a direct ab initio dynamics study, 17

Charge exchange

Mass spectra of Fe(CO)₅ using Fourier transform mass spectrometry (FTMS) and laser induced thermal desorption FTMS with electron ionization, charge exchange, and proton transfer, 83

Chemical ionization

Mass spectra of Fe(CO)₅ using Fourier transform mass spectrometry (FTMS) and laser induced thermal desorption FTMS with electron ionization, charge exchange, and proton transfer, 83

Chemical sputtering

Low-energy collisions of CF_3^+ ions with a hydrocarbon covered surface: Scattering, chemical sputtering, and reactive collisions, 105

Cluster

Generation of titanium oxide clusters of relatively large size, L1

Cluster formation reaction

Photoionization investigation of cluster formation in heterocyclic compounds and their reactions with acidic species, 197

Clusters

External source Fourier transform ion cyclotron resonance mass spectrometry by using a split-pair magnet, 63 Formation of antimony oxide clusters in a molecular beam. L5

Coincidence spectroscopy

Formation and dissociation of the nitric acid dication, 119 Collisional cooling

Relaxation of internally excited high-mass ions simulated under typical quadrupole ion trap storage conditions, 163 Cone jet

Pulsation phenomena during electrospray ionization, 1 Cross section

Electron capture and energy loss in \sim 100 keV collisions of atomic and molecular ions on C_{60} , 51

Density functional theory

Density functional study of mixed silicon carbide cluster cations $C_nSi_p^+$ (n + p = 5.6), 31

Desorption

Angular distribution of the ejecta in matrix-assisted laser desorption/ionization: Model dependence, 111

Direct ab initio dynamics

Formation mechanism of CCl₄⁻ anion in condensed phase: a direct ab initio dynamics study, 17

Direct laser vaporization

Generation of titanium oxide clusters of relatively large size, L1

Electron beam evaporation

Cooling of an incandescent filament by thermionic emission, 155

Electron capture

Electron capture and energy loss in \sim 100 keV collisions of atomic and molecular ions on C_{60} , 51

Electron ionization

Formation and dissociation of the nitric acid dication, 119 Kinetic energies of ions produced by dissociative electron impact ionization of propane, 143

Electrospray ionization

Pulsation phenomena during electrospray ionization, 1 Ligand-field photochemistry of the [Cu^{II}(bpy)(serine-H)]^{+•} complex in the gas phase, 187

Energy loss spectra

Electron capture and energy loss in ${\sim}100$ keV collisions of atomic and molecular ions on C_{60} , 51

Erbium

Absolute isotopic composition and atomic weight of erbium, 131

External ion source

External source Fourier transform ion cyclotron resonance mass spectrometry by using a split-pair magnet, 63

Filament

Cooling of an incandescent filament by thermionic emission, 155

Flowing afterglow

Simplified injector flanges for the selected ion flow tube, 175 Fourier transform

Characteristics of a broad-band Fourier transform ion mass spectrometer, 91

Fourier transform ion cyclotron resonance mass spectrometry

External source Fourier transform ion cyclotron resonance mass spectrometry by using a split-pair magnet, 63 Fragment ions

Kinetic energies of ions produced by dissociative electron impact ionization of propane, 143

Fullerene

Electron capture and energy loss in \sim 100 keV collisions of atomic and molecular ions on C_{60} , 51

Fullerene ions

New evidence in favor of a high (10 eV) C_2 binding energy in C_{60} , L9

H₂O in ice liquid

Ionizing collisions of electrons with H_2O molecules in ice and in water, 137

Helium bath gas

Relaxation of internally excited high-mass ions simulated under typical quadrupole ion trap storage conditions, 163 Heterocyclics

Photoionization investigation of cluster formation in heterocyclic compounds and their reactions with acidic species, 197

Inelastic cross sections

Ionizing collisions of electrons with H_2O molecules in ice and in water, 137

Injector flange

Simplified injector flanges for the selected ion flow tube, 175

Internal relaxation

Relaxation of internally excited high-mass ions simulated under typical quadrupole ion trap storage conditions, 163 Ionization cross sections

Improved low-energy dependence of calculated cross sections for the K-shell ionization of atoms using the Deutsch-Märk formalism, 47

Ion motion

Characteristics of a broad-band Fourier transform ion mass spectrometer, 91

Ion-neutral complexes

Decomposition of metastable methyl trifluoroacetate and ethyl trifluoroacetate upon electron impact, 23

Ion-surface reactions, CF₃⁺

Low-energy collisions of CF_3^+ ions with a hydrocarbon covered surface: Scattering, chemical sputtering, and reactive collisions, 105

Ion trap

Characteristics of a broad-band Fourier transform ion mass spectrometer, 91

Ion trap/reflectron

New evidence in favor of a high (10 eV) C_2 binding energy in C_{60} , L9

Iron pentacarbonyl

Mass spectra of Fe(CO)₅ using Fourier transform mass spectrometry (FTMS) and laser induced thermal desorption FTMS with electron ionization, charge exchange, and proton transfer, 83

Isotopic abundance

Absolute isotopic composition and atomic weight of erbium, 131

Kinetic energy

Kinetic energies of ions produced by dissociative electron impact ionization of propane, 143

K-shell ionization

Improved low-energy dependence of calculated cross sections for the K-shell ionization of atoms using the Deutsch-Märk formalism, 47

Laser

Angular distribution of the ejecta in matrix-assisted laser desorption/ionization: Model dependence, 111

Laser description thin layers

Influence of the substrate on the ion yield in direct laser desorption-ionization for thin organic layers, 217

Laser-induced thermal desorption

Mass spectra of Fe(CO)₅ using Fourier transform mass spectrometry (FTMS) and laser induced thermal desorption FTMS with electron ionization, charge exchange, and proton transfer, 83

MALDI

Angular distribution of the ejecta in matrix-assisted laser desorption/ionization: Model dependence, 111

Mass spectrometry

Density functional study of mixed silicon carbide cluster cations $C_nSi_p^+$ (n + p = 5,6), 31

Cooling of an incandescent filament by thermionic emission, 155

Metal oxides

Formation of antimony oxide clusters in a molecular beam, L5

Metastable fraction

New evidence in favor of a high (10 eV) C_2 binding energy in C_{60} , L9

Metastable ion

Decomposition of metastable methyl trifluoroacetate and ethyl trifluoroacetate upon electron impact, 23

MIKE

Decomposition of metastable methyl trifluoroacetate and ethyl trifluoroacetate upon electron impact, 23

Molecular beams

Formation of antimony oxide clusters in a molecular beam, L5

Nitric acid dication

Formation and dissociation of the nitric acid dication, 119 Nondestructive detection

Characteristics of a broad-band Fourier transform ion mass spectrometer, 91

Organofluorine compounds

Decomposition of metastable methyl trifluoroacetate and ethyl trifluoroacetate upon electron impact, 23

Photochemistry

Ligand-field photochemistry of the [Cu^{II}(bpy)(serine-H)]⁺ complex in the gas phase, 187

Photoionization

Photoionization investigation of cluster formation in heterocyclic compounds and their reactions with acidic species, 197

Propane

Kinetic energies of ions produced by dissociative electron impact ionization of propane, 143

Proton transfer

Mass spectra of $Fe(CO)_5$ using Fourier transform mass spectrometry (FTMS) and laser induced thermal desorption FTMS with electron ionization, charge exchange, and proton transfer, 83

Pulsation phenomena

Pulsation phenomena during electrospray ionization, 1

Quadrupole field

Characteristics of a broad-band Fourier transform ion mass spectrometer, 91

Quadrupole ion trap

Relaxation of internally excited high-mass ions simulated under typical quadrupole ion trap storage conditions, 163

Selected ion flow tube

Simplified injector flanges for the selected ion flow tube, 175 Semiempirical methods

Improved low-energy dependence of calculated cross sections for the K-shell ionization of atoms using the Deutsch-Märk formalism, 47

SIFT

Simplified injector flanges for the selected ion flow tube, 175 Silicon

Density functional study of mixed silicon carbide cluster cations $C_pSi_p^+$ (n + p = 5.6), 31

Silicone carbide

Density functional study of mixed silicon carbide cluster cations $C_n Si_p^+$ (n + p = 5,6), 31

Simulations

Characteristics of a broad-band Fourier transform ion mass spectrometer, 91

Spin density

Formation mechanism of CCl₄ anion in condensed phase: a direct ab initio dynamics study, 17

Split-pair magnet

External source Fourier transform ion cyclotron resonance mass spectrometry by using a split-pair magnet, 63 Structure elucidation

Formation of antimony oxide clusters in a molecular beam, L5

Tandem mass spectrometry

Low-energy collisions of CF_3^+ ions with a hydrocarbon covered surface: Scattering, chemical sputtering, and reactive collisions, 105

Temperature distribution

Cooling of an incandescent filament by thermionic emission, 155

Thermionic emission

Cooling of an incandescent filament by thermionic emission, 155

Time-of-flight

Influence of the substrate on the ion yield in direct laser desorption-ionization for thin organic layers, 217

Time-of-flight mass spectrometry

Formation and dissociation of the nitric acid dication, 119

Titanium oxide

Generation of titanium oxide clusters of relatively large size, L1

TOF mass spectrometer

Generation of titanium oxide clusters of relatively large size, L1

Trajectory

Formation mechanism of CCl₄⁻ anion in condensed phase: a direct ab initio dynamics study, 17

Transition-metal-ion complex

Ligand-field photochemistry of the $[Cu^{II}(bpy)(serine-H)]^{+\bullet}$ complex in the gas phase, 187

Venturi inlet

Simplified injector flanges for the selected ion flow tube, 175

Work function

Cooling of an incandescent filament by thermionic emission, 155